



SWIRLING FLOW VISUALIZATION IN BLOOD VESSELS AND ITS HYDRODYNAMIC MODELS

A.D. YUKHNEV^{1,c}, E.M. SMIRNOV¹, Y.S. CHUMAKOV¹, Y.A. GATAULIN¹,
V.P. KULIKOV², R.I. KIRSANOV²

¹Saint-Petersburg State Polytechnical University, Saint-Petersburg, 195251, Russia

²Altai State Medical University, Barnaul, 656031, Russia

^cCorresponding author: Tel.: +79119176550; Fax: +78125526621; Email: a.yukhnev@mail.ru

KEYWORDS:

Main subjects: *blood flow hydrodynamics*

Fluid: *swirling flow*

Visualization methods: *ultrasound color Doppler imaging, computational fluid dynamics*

Other keywords: *blood flow phantom*

ABSTRACT: *The present contribution is aimed at development of a quantitative ultrasound Doppler visualization technique in application to swirling flows. Methods of swirling blood flow velocity measurements in human arteries and its models are described. Flow visualization is performed both with the ultrasound color Doppler imaging mode and with CFD data post-processing of “etalon” swirling flows in a blood flow phantom. Decay of the maximal circumferential-to-maximal longitudinal velocity ratio as well as an integral swirl parameter downstream of a twisted tape is evaluated. Using results of “etalon” flow calculations, principal errors of the measurement technique developed are estimated.*

1. INTRODUCTION

For a long time, understanding of swirling (helical) blood flow was pure and based on data for morphological structure of the heart and large vessels. It was assumed in particular that helical blood flows were caused by the spiral arrangement of muscle elements in the blood vessel wall [1] and/or by the twisting nature of cardiac muscle contraction [2,3]. Numerous experimental studies performed recently have allowed to register the helical blood flow in different parts of the cardiovascular system using such methods as the radiopaque angiography [4], the ultrasound color flow imaging [5] and the phase-contrast magnetic resonance angiography [6-9]. But majorities of data on helical blood flows are of qualitative character. Only few works present quantitative parameters of the swirling flow measured by phase-contrast magnetic resonance angiography in the aortic arch [10, 11]. The role of the helical blood flow in development of vascular pathology remains unclear. On the one hand, some researchers suggest that the swirl affects positively blood circulation [12] and protects vascular wall from atherosclerotic lesions [13,14]. On the other hand, the swirling blood flow might play a pathogenetic role in atherogenesis [15,16]. Without a deep knowledge of peculiarities and quantitative parameters of swirling blood flow it is impossible to estimate biological and clinical significance of the swirl.

The majority of modern clinical data concerning swirl flow have been obtained using the phase-contrast magnetic resonance technique. There are only few studies that report registration of swirling blood flow using the ultrasound technique. However, employment of the ultrasound Doppler method is the most common and affordable way of estimating the blood flow parameters, and it is very attractive to use this method for measuring swirling blood flow during diagnostics of vascular diseases and for assessment of results of vascular reconstructive operations, including those that use artificial prosthesis [17].

The aim of the present work is development of a quantitative visualization technique based on the ultrasound Doppler method with application to swirling flows in blood vessels on the base of blood flow phantom measurements and comparisons with visualization of computational fluid dynamics data obtained for phantom vessel models.

2. ULTRASOUND VISUALIZATION AND QUANTITATIVE EVALUATION OF SWIRLING BLOOD FLOW IN HUMAN ARTERIES

Swirling blood flow registration and estimation method using the ultrasound Doppler technique was developed and applied by the authors [18,19]. This method allows to register the circumferential component of blood velocity and to evaluate swirl intensity. Blood flow circumferential component registration is realized by scanning an artery cross section in the Color Doppler Imaging mode (CDI). Different coloring of the blood flow (red and blue) in lateral and medial hemicircles of an artery cross section testifies swirling blood flow (Fig. 1a).



Blood flow swirling quantitative evaluation includes measuring longitudinal, circumferential and radial velocity components. The longitudinal velocity component is measured in color Duplex imaging mode by registering impulse-wave Doppler spectra in artery longitudinal section using a traditional technique (Fig. 1b).

The circumferential velocity component evaluation is carried out in the color Duplex imaging mode by registering impulse-wave Doppler spectra in an artery cross section, with a sample volume placed in turns into the lateral and medial hemicircles of the artery lumen (Fig. 1c). The sample volume size corresponds to vessel radius, and the angle between the blood flow direction and the ultrasound beam is set to 0°. Circumferential velocity of the blood flow is measured for each position of the sample volume with the following averaging of the circumferential velocity values between the lateral and medial hemicircles of the artery.

The radial velocity component is measured in the M-mode by means of estimating the ratio of the artery radius augmentation to the time of this augmentation while pulse wave is passing.

Magnitude velocity of swirling blood flow, V , is estimated as $V = (V_z^2 + V_\phi^2 + V_r^2)^{1/2}$, where V_z is the longitudinal velocity component, V_ϕ circumferential velocity component and V_r radial velocity component.

With the help of this method the authors estimated the flow velocity vector and its components for carotid arteries [20,21]. However this method needs to be modified as far as Doppler measurement results depend on the angle between the blood flow direction and the ultrasound beam, and the blood flow helix angle is unknown a priori. That is why estimation of the circumferential velocity can be inaccurate. Accuracy of the swirling flow parameters obtained by the Doppler ultrasound method has to be checked with a calibrating device (blood flow phantom) that can result in optimization of the method.

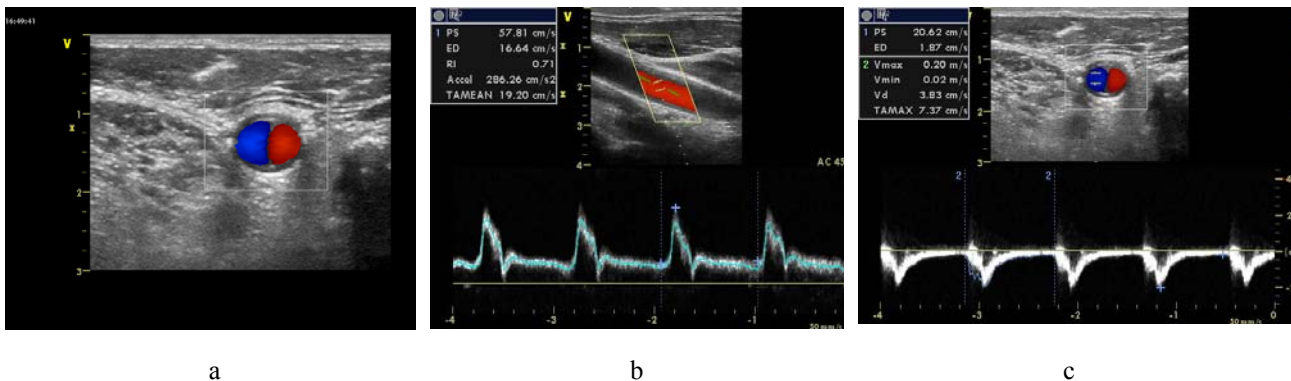


Fig.1 Doppler ultrasound visualization of swirling blood flow in a human common carotid artery: a – blood flow circumferential velocity component registration in CDI (red and blue coloring of blood flow in lateral and medial hemicircles of an artery cross section), b – evaluation of longitudinal velocity component in color Duplex imaging mode (at the top – image of artery longitudinal section, at the bottom – impulse-wave Doppler spectra of blood flow), c – evaluation of circumferential velocity component in color Duplex imaging mode (sample volume is placed in left half of artery lumen, Doppler spectra is below the base line)

3. NUMERICAL SIMULATION OF SWIRLING FLOW IN A BLOOD VESSEL MODEL

To obtain a base for estimation of accuracy of blood flow swirl measurements with the ultrasound Doppler method, numerical simulation of steady-state three-dimensional swirling flow in a vessel model was carried out [22]. For the vessel model considered in the present work, geometry and boundary conditions correspond to a physical prototype implemented in the blood flow phantom. Uniform velocity V_{mean} is prescribed at the model inlet. Incompressible fluid with the kinematic viscosity of $2 \cdot 10^{-6} \text{ m}^2/\text{s}$ passes through a twisted tape, 20 mm length and 0.4 mm thickness, inserted into the vessel model of circular cross-section, 6 mm diameter and 100 mm length. The twisted tape has the inlet-to-outlet angle of 180°. All calculations were performed with the ANSYS CFX v.12.0 software. Geometry and grids were built in ICEM CFD v.12. The basic grid used consisted of about 600,000 cells. As result of a grid sensitivity study, the solution obtained with this grid is treated as a grid independent. Below it is used as an “etalon” for evaluation of errors inherent to the ultrasound Doppler measurement technique under development.

Some results of numerical simulation performed with $V_{\text{mean}} = 0.15, 0.32, 0.65 \text{ m/s}$ are given in Table 1. The Reynolds numbers, based of the vessel inner diameter and the mean velocity, are 450, 960, 1950 correspondingly. Values of the calculated velocities, swirl angle and two dimensionless swirl parameters are given for the cross-section positioned at $Z/D=5$ ($Z=0$ corresponds to the twisted tape outlet edge).



Table 1. Computed swirling flow parameters at section Z/D=5

| V_{mean} m/s | $V_{z\ max}$ m/s | $V_{\phi\ max}$ m/s | $V_{\phi\ max} / V_{z\ max}$ | S | α_{mean} deg |
|-------------------|---------------------|------------------------|------------------------------|------|------------------------|
| 0,15 | 0,25 | 0,04 | 0,16 | 0,08 | 7,7 |
| 0,32 | 0,54 | 0,11 | 0,20 | 0,11 | 10,4 |
| 0,65 | 1,07 | 0,24 | 0,22 | 0,13 | 12,1 |

The integral swirl parameter, S, is defined as the ratio of the flux of moment of circumferential momentum to the product of the axial momentum flux and the vessel radius R

$$S = \frac{\int_0^R V_{\phi} V_z r^2 dr}{\left(R \int_0^R V_z^2 r dr \right)} \quad (1),$$

and α_{mean} is the area-averaged swirl flow angle

$$\alpha_{mean} = \frac{1}{A} \int \arctg \left(\frac{V_{\phi}}{V_z} \right) dA \quad (2).$$

Swirling flow in the blood flow phantom can be divided into two regions: initial, $Z < L_0 = 5D$, and main. In the initial region, flow field is of complex structure and sensitive to the inlet conditions imposed upstream of the twisted tape. In the main region, the inlet conditions do not affect evolution of the swirling flow in the streamwise direction. For the case of $V_{mean} = 0.32$ m/s, flow features are illustrated in Figs. 2-3.

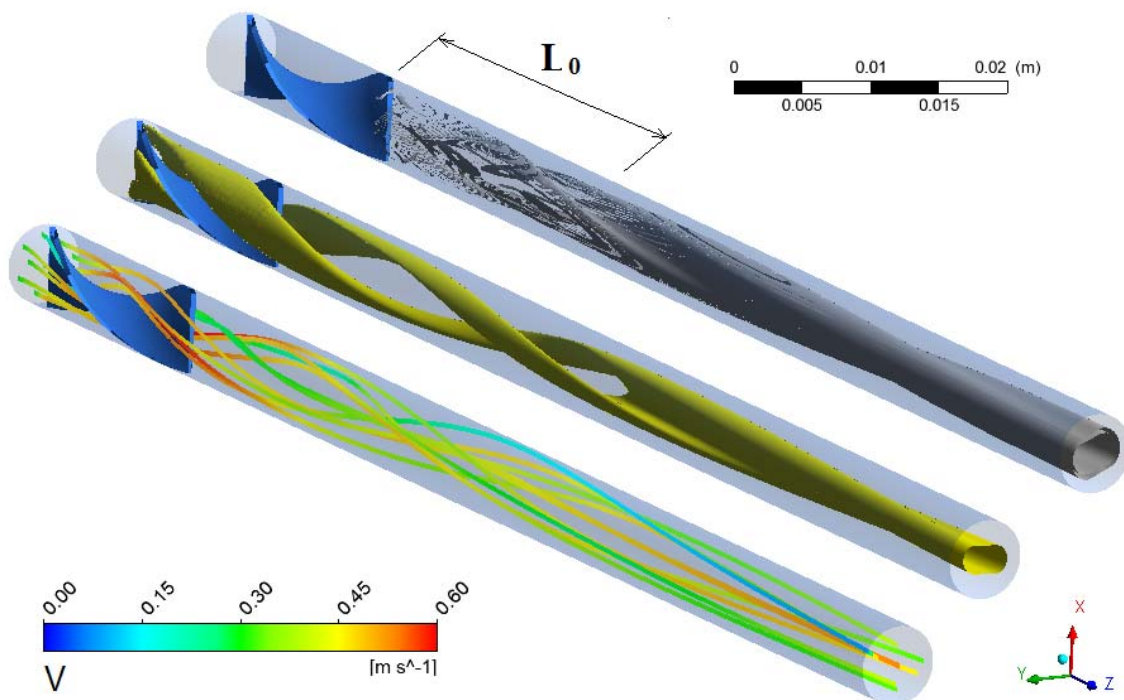


Fig.2 From top to bottom: vorticity Z-component isosurface, longitudinal velocity isosurface and swirling flow streamlines colored by velocity magnitude (computations at $V_{mean} = 0.32$ m/s)



Cross-section distributions of the circumferential and longitudinal velocity components differ significantly in the initial and the main region (Fig. 3). In the initial “two-jets” region two peaks of the longitudinal velocity are observed. In the main region where the jets are merged, there is only one maximum of the longitudinal velocity. Remarkably that overall the vessel model streamwise variation of the maximum longitudinal velocity is non-monotonic. On the contrary, maximum value of the circumferential velocity decreases monotonically downstream of the twisted-tape region outlet.

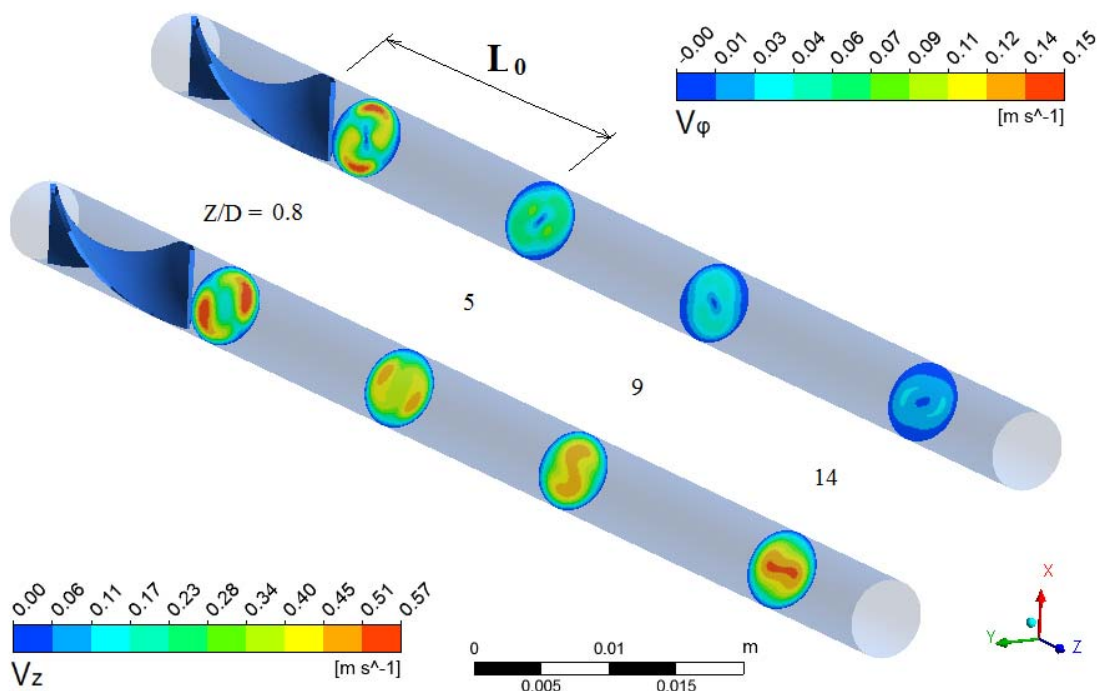


Fig 3. Distributions of the circumferential and longitudinal velocity components over various cross sections of the vessel model (computations at $V_{\text{mean}} = 0.32$ m/s)

4. BLOOD FLOW PHANTOM AND ERROR ESTIMATIONS OF ULTRASOUND DOPPLER MEASUREMENTS OF SWIRLING FLOW

As mentioned in Section 2, accuracy of the swirling flow parameters obtained by the Doppler ultrasound method has to be checked with a specialized calibrating device. Using the experience accumulated previously [23], a blood flow phantom for producing “etalon” swirling flows was designed, assembled and calibrated. Generally, with the phantom one is able to produce “etalon” steady-state and pulsating flows of blood mimicking fluid and to simulate propagation of ultrasound wave in biological tissues. It consists of a container with vessels models laid in tissue mimicking material and an electronically-controlled pump producing flow rate ranged from 0 to 0.5 l/min with 0 to 2 Hz pulse frequency (Fig. 4).

Two of the four vessel models can be supplemented by a swirl generator of twisted-tape kind (made of plastic). Twisted tapes with angles of 180°, 270° and 360° between the input and output edges can be installed. Models of the vessel are made of silicone tubing, either cylindrical or with local contraction in the form of stenosis. Different models of stenoses, hemodynamically insignificant (30% by area), light (50%), moderate (70%) and severe (80%), can be installed in phantom. The container upper part is closed with a thin elastic film that is a skin simulator. At the front of the flow phantom there is a rectangular frame that allows filling the surface of the skin simulator with water, thus providing acoustic contact with an ultrasound Doppler transducer. The phantom measurements are performed using a linear transducer and a standard program (Echo Wave II) of ultrasound scanner LogicScan 64. The scanner operates in full duplex mode: gray-scale, color Doppler imaging and pulsed-wave Doppler mode.

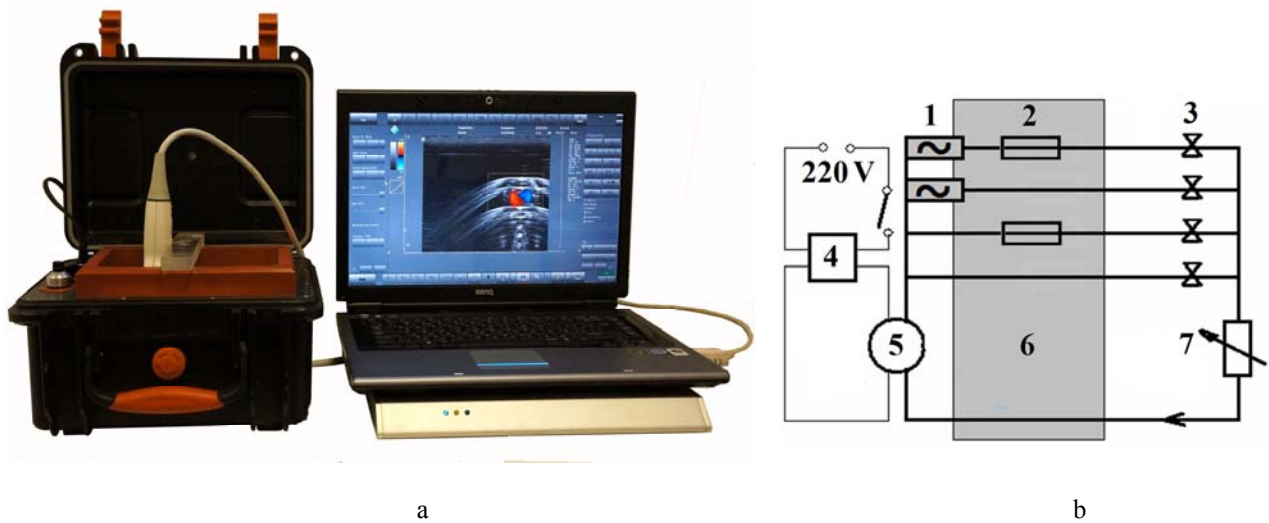


Fig.4 Blood flow phantom with ultrasound scanner LogicScan 64: a – overview, b – phantom scheme;
1 – twisted-tape swirl generator, 2 – model of vascular stenosis, 3 – valve, 4 – frequency controller, 5 - pump,
6 - container with tissue mimicking material, 7 - flow rate controller

Consider the usage of the ultrasound Doppler technique for measuring the velocity of blood flow in the phantom focusing at evaluation of the maximum circumferential, $V_{\phi \max}$, and the maximum longitudinal velocity, $V_{z \max}$ in the main region of swirling flow.

Measurement of the maximum longitudinal velocity $V_{z \max}$ component is carried out as follows:

- the transducer is installed in section $Z = Z_0$, with the θ angle between the transducer axis and the vessel axis, and the axis of the vessel model lies in the scanning plane (Fig. 5.a);
- size of the sample volume is set equal to the vessel model diameter;
- center of the sample volume is set to the point with coordinates $Z = Z_0, X = 0, Y = 0$;
- Doppler angle is set equal to θ ;
- the scanner software automatically calculates the maximum value of velocity $V_{z \max US}$ in the sample volume that is approximately equal to the maximum longitudinal velocity component $V_{z \max}$.

Measurement of the maximum circumferential velocity component $V_{\phi \max}$ is carried out as follows:

- the transducer is installed in section $Z = Z_0$, the scanning plane and hence the transducer axis are perpendicular to the vessel model axis (Fig. 5.b);
- size of the sample volume is set equal to the vessel model radius;
- center of the sample volume is set first to the left side of the vessel to the point with coordinates $X = -0.5R, Y = 0$;
- Doppler angle is set equal to 0;
- the scanner software automatically calculates the maximum velocity $V_{\phi \max US1}$;
- center of the sample volume is set in the right half of the vessel to the point with the coordinates $X = 0.5R, Y = 0$;
- the scanner software automatically calculates the absolute maximum velocity $V_{\phi \max US2}$;
- the maximum circumferential velocity component is approximately calculated as the average of the absolute values of the measured maximum velocities in the left and right halves of the vessel: $V_{\phi \max} \approx 0.5 (V_{\phi \max US1} + V_{\phi \max US2})$.

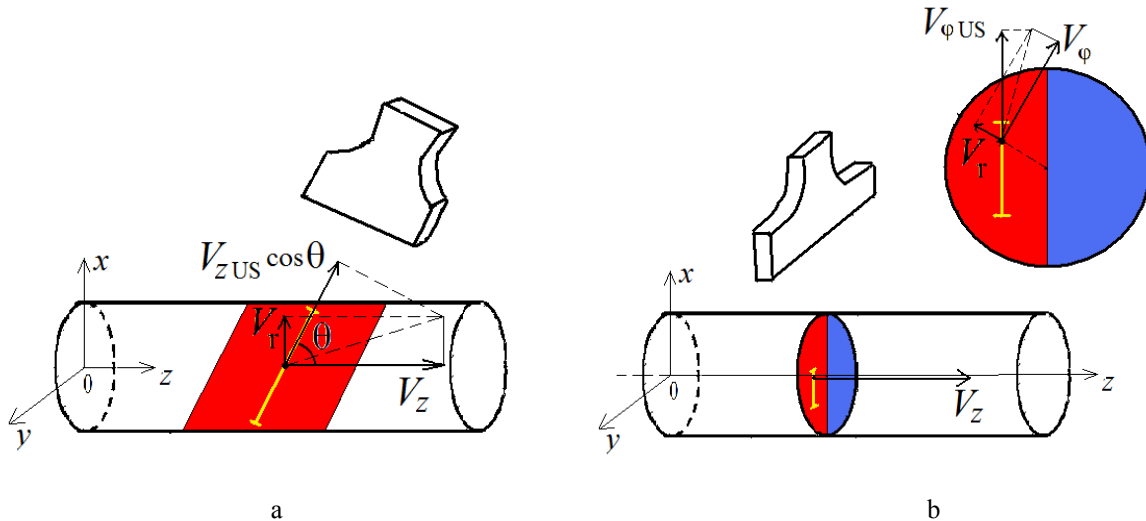


Fig.5 Schemes of the ultrasound scanner transducer positions during measurements of swirling flow:
a – at measurements of maximum longitudinal velocity the axis of the vessel model lies in scanning plane and transducer axis has angle θ less than 90° with vessel model axis, b - at measurements of maximum circumferential velocity the scanning plane and transducer axis is perpendicular to vessel model axis

For ultrasound Doppler technique described above, numerical estimation of two velocities measurement errors was performed. It points that measurement of the maximum circumferential velocity component is of the highest accuracy if the maximum circumferential velocity component is closer to the diameter perpendicular to transducer axis (Fig. 6). The relative error in measuring the circumferential velocity component is calculated by the formula $\delta V_\phi = (|V_\phi - |V_{\phi US}|) / |V_\phi| \cdot 100\%$. In the main region calculated error does not exceed 20%. The error caused by mismatched components of the velocity directions of the unit vector and the axis of the transducer, as well as presence of a nonzero radial velocity component.

The relative difference between the calculated and measured longitudinal velocity component is calculated by the formula $\delta V_z = (|V_z - V_{z US}|) / |V_z| \cdot 100\%$. In the main region of swirling flow calculated measurement error does not exceed 30% (Fig. 7). The error is caused by presence of non-zero radial velocity component.

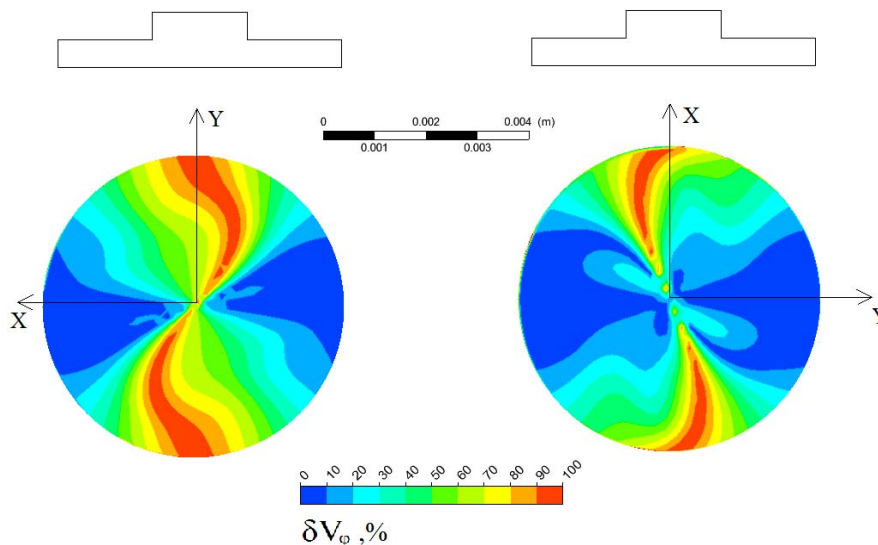


Fig. 6. Example of calculated relative error estimation in measurements of circumferential velocity component, error is caused by mismatch between directions of this component unit vector and transducer axis, as well as presence of nonzero radial velocity component (computations at $Z / D = 5$, $V_{mean} = 0.32$ m/s)

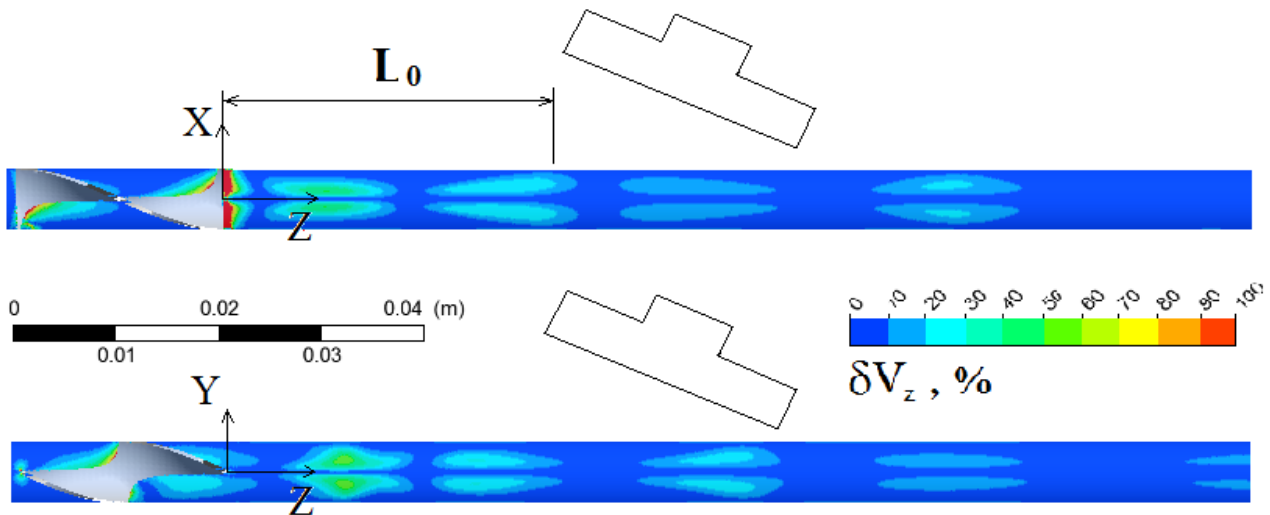


Fig.7 Example of calculated relative error estimation in measurements of longitudinal velocity component, error is caused by presence of nonzero radial velocity component (computations at $V_{\text{mean}} = 0.32$ m/s)

5. COMPARISON OF NUMERICAL AND EXPERIMENTAL RESULTS

Experimental data are presented in the form of ultrasound images obtained by the LogicScan 64 scanner color flow mapping mode for non-swirling (Fig. 8) and swirling flows (Fig. 9-11) in vascular models at two positions of the scanning plane. The images are processed the original image-processing program with the construction of the velocity distribution in the color and scale, corresponding to the results of numerical calculations (Fig. 10). Numerical results are presented in the form of distributions of the velocity vector projections of swirling flow in the direction of the axis of the ultrasonic transducer (Fig. 11). Experimental and theoretical results provide a qualitative agreement between the structures of swirling flow.

Figure 12.a shows the maximal circumferential-to-the maximal longitudinal velocity ratio vs longitudinal coordinate and flow rate. Discordance of the results does not exceed 10% for high velocities and up to 60% for the low-velocity weak swirling flow. Figure 12.b shows that this ratio decreases uniformly downstream and increases with increasing flow rate through the inlet twisted tape similar to the integral swirling flow parameter.

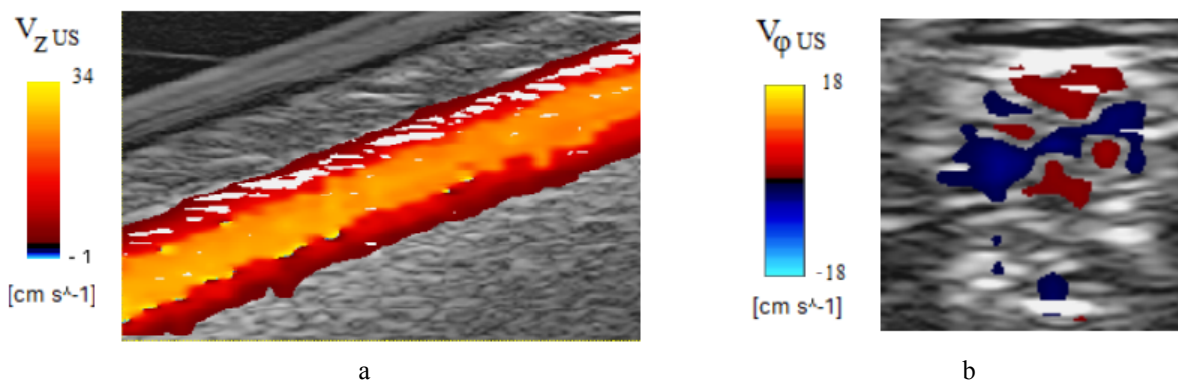


Fig.8 Ultrasound color flow imaging of non-swirling flow in vessel model: a - longitudinal velocity pattern, b - cross section velocity pattern ($V_{\text{mean}} = 0.32$ m/s, $Z/D = 5$)

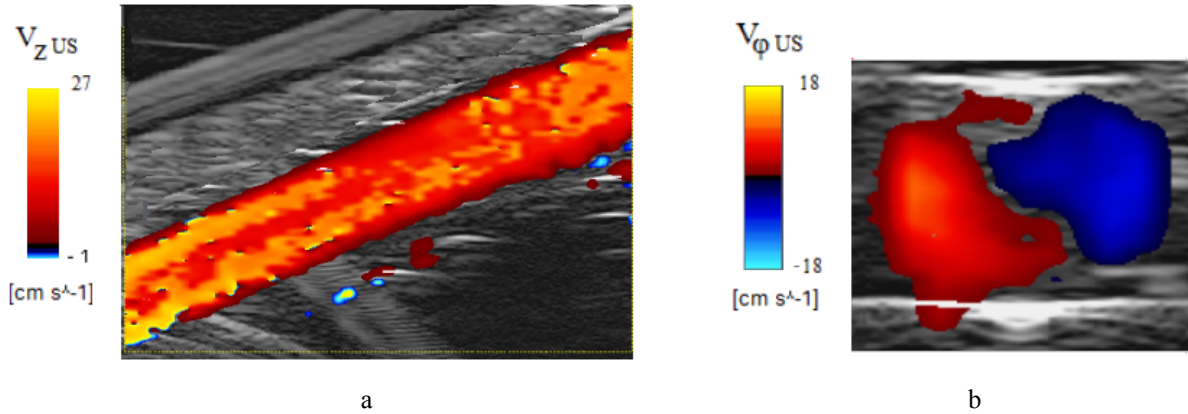


Fig.9 Ultrasound color flow imaging of swirling flow in vessel model: a - longitudinal velocity pattern, b - cross section velocity pattern ($V_{\text{mean}} = 0.32 \text{ m/s}$, $Z/D = 5$)

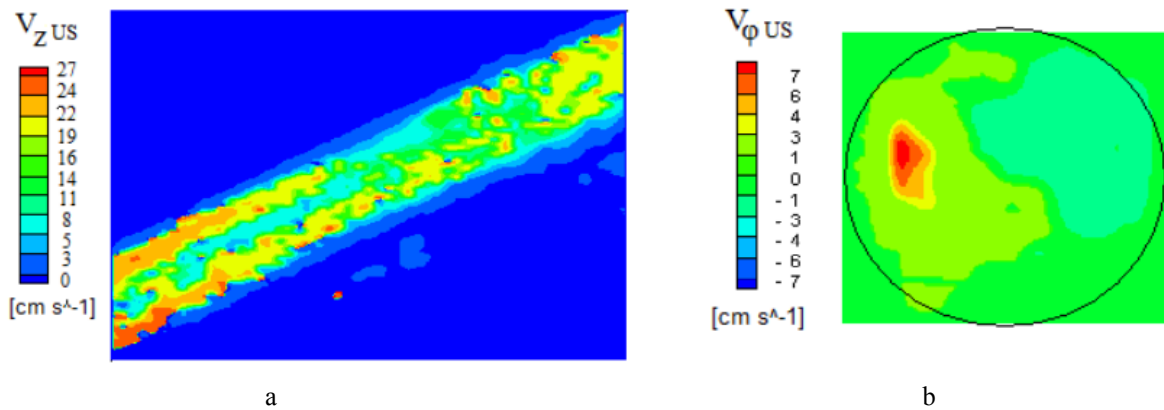


Fig.10 Digitized ultrasound color flow images from Fig. 9

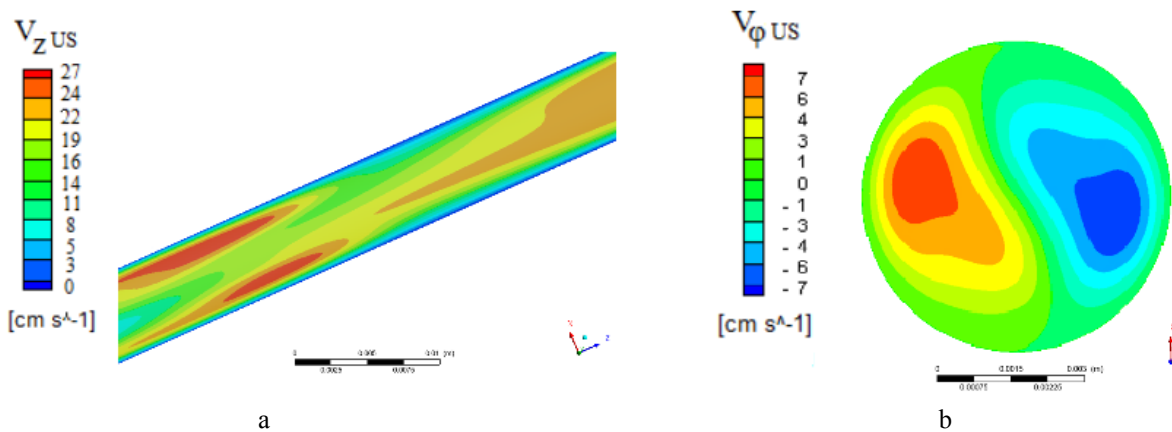


Fig.11 Visualization of swirling flow calculations corresponding to the developed visualization technique

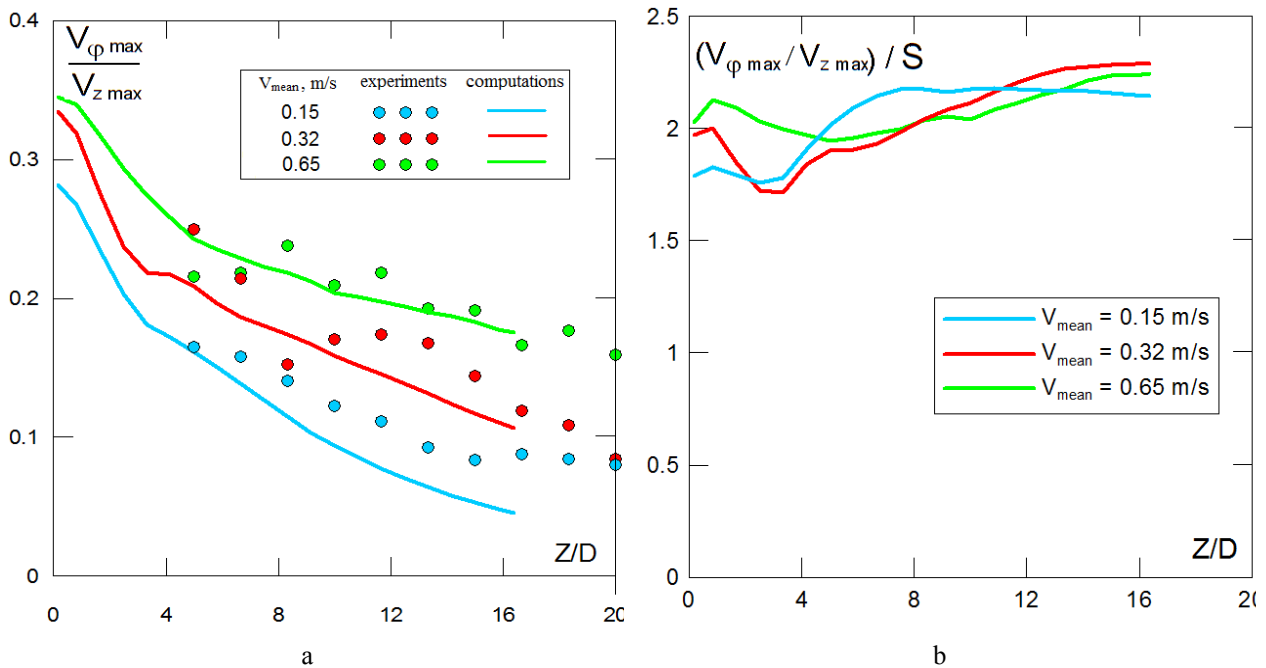


Fig.12 Swirl flow parameters vs. longitudinal coordinate and flow rate:

a - measured and calculated the maximal circumferential-to-the maximal longitudinal velocity ratio, b – calculated the above ratio divided by the integral swirl parameter

CONCLUSIONS

Combining numerical and physical modeling of “etalon” swirling flows, a considerable progress in development of quantitative ultrasound swirling flow visualization has been achieved. Using a blood flow phantom with modern medical ultrasound scanners allows handling a technique of quantitative visualization of swirling flows by comparing ultrasound images with CFD-generated analogues.

CFD solutions showed that the ratio of the maximum circumferential and the maximum longitudinal velocity, $V_{\phi \max} / V_{z \max}$, adequately describes the decay of the swirl intensity along the vessel model. These velocities can be measured with the ultrasound Doppler technique with a proper accuracy. It has been estimated that measurement error of circumferential velocity component in the flow main region does not exceed 20%, and longitudinal - 30%. The errors are caused mainly by mismatch of the circumferential directions of the unit vector components and the transducer axis, as well as by presence of the radial velocity component. Distinctions in calculated and measured velocity ratio $V_{\phi \max} / V_{z \max}$ does not exceed 20%.

Further developments of the synthetic method suggested will be aimed at its extension to quantitative ultrasound Doppler visualization of more complex flows, such as swirling pulsating flows in vessels with local contractions and elastic walls.

ACKNOWLEDGMENTS

Authors would like express their thanks to Russian Foundation for Basic Research for support of the work under grant №12-01-00910 «Swirling blood flow in vessels with atherosclerotic lesions: simulation and diagnostics».

REFERENCES

1. Kupriyanov V.V. *Spiral arrangement of elements in the muscle wall of blood vessels and its significance for hemodynamics. Archives of Anatomy, Histology and Embryology.* 1983. - **LXXXV** (9): p. 46-54 (in Russian)
2. Sengupta P.P. Krishnamoorthy V.K., Korinek J. et al. *Left ventricular form and function revisited: applied translational science to cardiovascular ultrasound imaging.* J. Am. Soc. Echocardiogr. 2007, **20** (5), p. 539-551 (in Russian)
3. Bagaev S.N. et al. *The need for helical motion of blood.* Russian J. Biomech. 2002, **6** (4), p. 30-51 (in Russian)
4. Frazin L. et al. *Functional chiral asymmetry in descending thoracic aorta.* Circulation, 1990, **82**(6), p. 1985-1994



5. Bokeria L.A., Borouhgs A.Yu., Nikolaev D.A. etc. *The analysis of the velocity field of swirling blood flow in the aorta on the basis of three-dimensional mapping with magnetic resonance velocimetry*. Bulletin of Research Center on Cardiovascular Surgery named after A.N. Bakulev of RAMS. Cardiovascular Diseases. 2003, 4 (9), p. 70-74 (in Russian)
6. Tulupov A.A., Saveliev L.A., Gorev V.N. *Functional analysis of the venous outflow from the brain in normal conditions with magnetic resonance imaging*. Clinical Physiology of Circulation. 2009, 2, p. 65-70 (in Russian)
7. Bogren H. et al. *4D magnetic resonance velocity mapping of blood flow patterns in the aorta in young vs. elderly normal subjects*. J. Magn. Reson. Imaging. 1999, 10, p. 861-869
8. Mark M. et al. *Time-resolved three-dimensional magnetic resonance velocity mapping of aortic flow in healthy volunteers and patients after valve-sparing aortic root replacement*. J. Thorac. Cardiovasc. Surg. 2005, **130**, p. 456-463.
9. Kilner P. et al. *Helical and retrograde secondary flow patterns in the aortic arch studied by three-directional magnetic resonance velocity mapping*. Circulation. 1993, **88** (5), Pt.1, p. 2235-2247
10. Houston J.G. et al. *Two-dimensional flow quantitative MRI of aortic arch blood flow patterns: effect of age, sex and presence of carotid athermanous disease on prevalence of spiral blood flow*. J. Magn. Reson. Imaging. 2003, **8**, p. 169-174
11. Stonebridge P.A. *Three-dimensional blood flow dynamics: spiral/helical laminar flow*. DeBakey Cardiovascular Journal. 2011, **8**(1), p. 21-26
12. Houston J.G. et al. *Spiral laminar flow in the abdominal aorta: a predictor of renal impairment deterioration in patients with renal artery stenosis?* Nephrol. Dial. Transplant. 2004, **19**, p. 1786-1791
13. Shinke T. et al. *Novel helical stent design elicits swirling blood flow pattern and inhibits neointima formation in porcine carotid arteries*. Circulation. 2008, **118**, p. 1054
14. Pritchard W. et al. *Effects of wall shear stress and fluid recirculation on the localization of circulating monocytes in a three-dimensional flow model*. J. Biomech. 1995, **28**(12), p. 1459-1469
15. Wensing P. et al. *Early atherosclerotic lesions spiraling through the femoral artery*. Arterioscler. Thromb. Vasc. Biol. – 1998. 18 (10) p. 1554-1558.
16. *Ultrasound diagnosis of vascular diseases*. Ed. V.P. Kulikov - STROM. 2007 (in Russian)
17. Orlovsky P.I., Uglov F.G., Bushmarin O.N., Yukhnev A.D. et al. *Should we take into account a presence of swirling blood flow in the left ventricle of heart and in the aorta for constructing artificial heart valves?* Vestnik of Surgery. 1998, **157** (1), p. 10-16 (in Russian)
18. Kulikov V.P., Kirsanov R.I. *Basic laws of blood screw motion in human common carotid arteries*. Russian J. of Physiology, 2008, **94**(8), p. 900-908 (in Russian)
19. Kulikov V.P., Kirsanov R.I. *Method of helical blood flow velocity measurement in human arteries*. Patent RU № 2380040, 27.07.2008 (in Russian)
20. Kulikov V.P., Kirsanov R.I. *Objective Laws and Quantitative Value of Helical Blood Flow in Precerebral Arteries (Chapter 4)* // In: Advances Medicine and Biology. V.8 / Ed. by L.V.Berhardt. New York: Nova Science Publishers. 2010, p. 129-163
21. Kirsanov R.I. *Dopplerography method of registration and quantitative assessment of the helical blood flow in human arteries*. Ultrasound & Functional Diagnostics. 2011, 6, p. 111-119 (in Russian)
22. Gataulin Y.A., Yukhnev A.D. *Numerical simulation of flows in stenosed blood vessel: influence of elasticity and flow swirl*. Vestnik of Lobachevsky State University of Nizhni Novgorod. 2011, №4, pt.5, p.2095-2096 (in Russian)
23. Yukhnev A.D., Chumakov Yu.S. et al. *Experience of experimental modeling of blood hydrodynamics*. Clinical Physiology of Circulation. 2009, 4, p. 15-21 (in Russian)